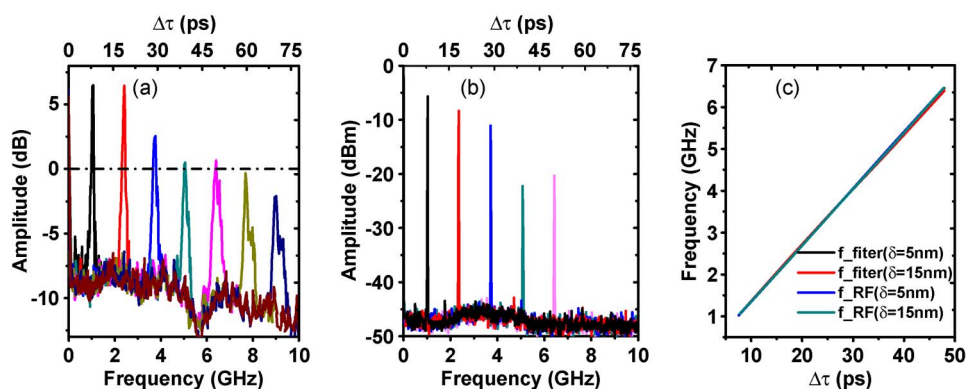# An Optoelectronic Oscillator Based on Carrier-Suppression-Effect-Free Single Bandpass Microwave Photonic Filter

Chenjun Liu
Weiwen Zou
Jianping Chen

An Optoelectronic Oscillator Based on Carrier-Suppression-Effect-Free Single Bandpass Microwave Photonic Filter

Chenjun Liu, Weiwen Zou, and Jianping Chen

State Key Laboratory of Advanced Optical Communication Systems and Networks, Department of Electronic Engineering, Shanghai Jiao Tong University, Shanghai 200240, China

Abstract: A novel optoelectronic oscillator based on a single bandpass microwave photonic filter (MPF) without any electronic microwave filter is proposed and experimentally demonstrated. The MPF, which is composed by a broadband optical source, an inline interferometer based on a variable optical delay line (VODL), an intensity modulator, and a dispersive element, serves as an oscillating mode selector. The oscillation frequency can be tuned by changing the differential time delay via the VODL. Due to the non-carrier-suppression effect of the selector, the oscillator can generate transmission-null-free microwave signal with widely tunable frequency range. An experiment is performed, and a tunable frequency range of 6.8 GHz is achieved. The generated microwave signal at $\sim$6.5 GHz ($\sim$1.06 GHz) exhibits a good phase noise performance about -95 dBc/Hz (-110 dBc/Hz) at an offset of 10 kHz.

Index Terms: Optoelectronic oscillator, microwave photonic filter, carrier suppression effect, decay effect.

1. Introduction

Optoelectronic oscillator (OEO) has attracted great interests for generating largely tunable and low phase-noise microwave signal [1], and it reveals wide applications in optical signal processing, radar, and radio over fiber system. Conventional oscillators are based on electronic techniques employing microwave filters to select one mode to achieve high spectral purity [2]. These filters are nevertheless limited by the achievable high quality factor (Q), largely tunable frequency range and high tuning speed. To overcome these limitations, microwave photonic filters (MPFs) are commonly used to perform the mode selection, and bring the advantages over electronic microwave filters such as low loss, high Q, immunity to electromagnetic interferences, large tunability and reconfigurability [3], [4]. During the last decade, a great number of approaches have been applied to achieve high-performance MPFs. Most of them have a non-desired periodic spectral characteristics and limited in many RF applications. Up to date, the slicing approach with fiber Mach–Zehnder interferometer (MZI) was demonstrated to be effective to achieve single bandpass performance since the output of MZI shows sinusoidal and continuous optical samples, and its weight distribution allows obtaining a single bandpass filter response. However, photonic microwave tunable single bandpass filter based on a MZI [5] encounters the so-called carrier-suppression effect (CSE) due to the double sideband
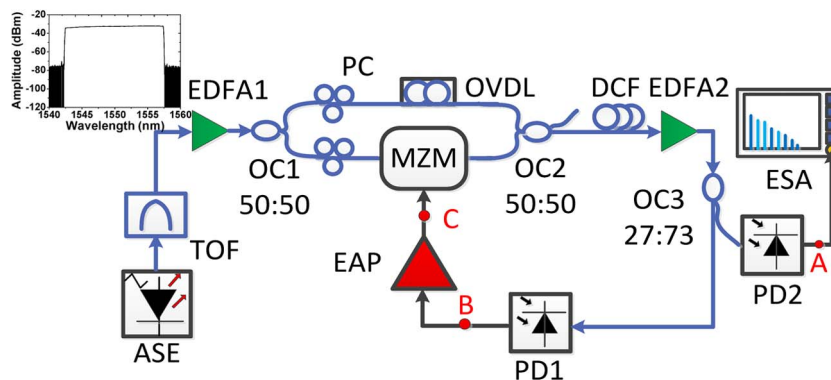
Fig. 1. Schematic of the proposed optoelectronic oscillator. TOF, tunable optical filter; PC, polarization controller; OC, optical coupler; DCF, dispersion compensation fiber; MZM, Mach–Zehnder modulator; PD, photo detector; VODL, variable optical delay line, ESA, electrical spectrum analyzer; EAP, electrical amplifier.

modulation and RF decay effects [5], [9] resulting from the dispersive slope of the dispersive medium. Alternative modulation as single-side band modulation can be used to avoid CSE [5], but the complexity of the system is increased. Xue *et al.* [8] came up with MPF by using a non-sliced broadband optical source, which can fulfill single bandpass performance and be free from the CSE without single-sideband modulation or phase modulation.

Yao *et al.* reported kinds of MPFs to implement OEO [3], [10], [11], [13], which can tune frequency by detuning of the wavelength of the laser, but also suffer the instability owing to the wavelength drift of the laser source. Although the tunable OEO incorporating the spectrum-sliced photonic microwave transversal filter was proposed, it is limited by the carrier-suppression effect (CSE) and cannot be continually transmission-null-free tuned [12], [13].

In this paper, we propose and experimentally demonstrate a new OEO based on a broadband optical source (BOS) and an inline MZI composing a variable optical delay line (VODL) and an intensity modulator. The combined BOS and MZI structure was recently proved to be effective to achieve a tunable single bandpass MPF [8]. Further analysis on the effect of dispersive slope on the amplitude response of the MPF is presented. The OEO possesses the merits of high frequency oscillation and transmission-null-free wide frequency tuning range.

2. Setup and Operating Principle

Fig. 1 shows the schematic of the proposed OEO. An ASE source is reshaped by a BOS and amplified by an EDFA1, which is split into two parts by a 50/50 coupler. One part (upper) is delayed with a variable optical delay line (VODL); the second part (lower) is modulated by a Mach–Zehnder modulator (MZM). The two parts have the same polarization states optimized by two polarization controllers (PCs) and are coupled together by the other 50/50 coupler. The structure formed by those two couplers and the related components offers a tunable inline MZI. Its output is directed into a dispersion compensation fiber (DCF) served as a dispersive element and then converted to an electrical signal by two photo-detectors (PD1 and PD2).

To meet the oscillating condition, the small-signal open-loop gain must be larger than unity, i.e., $G > 1$. Therefore, we insert another EDFA2 just after the DCF. To improve the RF gain and reduce the noise figure of the link [14], the MZM is low-biased other than quadrature-biased case. Finally, a 27/73 coupler (OC3) is applied to overcome the saturation of the PD1 and further split 73% optical power to another PD (PD2) served as the RF output.

To study the response of the open-loop OEO disconnected at the "A" and "B" in Fig. 1, it is assumed that the MZM is driven by an electrical signal with a frequency f_c, and the microwave-modulated optical signal is then directed into the dispersive element. The filtered optical broadband source, the MZM, the VODL, and the dispersive element (DCF) effectively can work as
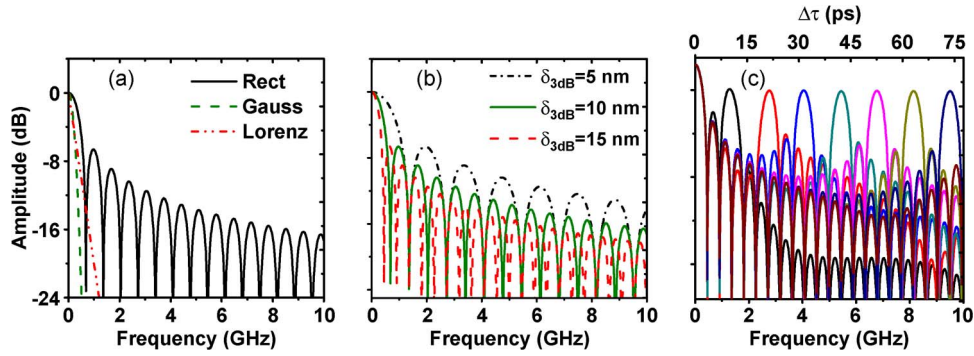
Fig. 2. (a) $H_b(\omega)$ under different BOS profile. (b) $H_b(\omega)$ for different $\delta_{3\,dB}$ of BOS. (c) $H(\omega)$ for different $\Delta\tau$ (i.e., different frequency shown in different color) with the $\delta_{3\,dB} = 15$ nm rectangular BOS profile.

a single bandpass MPF [8], which will function to select the wanted microwave frequency in the proposed OEO.

The phase delay $\Phi(\Omega)$ resulting from the DCF can be approximately written in a Taylor expansion at the center angular frequency (Ω_0) of the BOS like $\Omega_0\Phi(\Omega) = \beta_0 + \beta_1(\Omega - \Omega_0) + \beta_2(\Omega - \Omega_0)^2/2 + \beta_3(\Omega - \Omega_0)^3/6$. Ignoring the third-order dispersion β_3 and the baseband response, the MPF's transfer function (i.e., the amplitude response) can be described as [9]

$$H(\omega) \propto \exp\left[j(\Omega_0\Delta\tau - \beta_2\omega^2/2)\right] \times H_b(\omega - \Delta\tau/\beta_2)$$
$$+ \exp\left[j(-\Omega_0\Delta\tau + \beta_2\omega^2/2)\right] \times H_b(\omega + \Delta\tau/\beta_2) \quad (1)$$

where $H_b(\omega)$ is defined by

$$H_b(\omega) = \frac{1}{2\pi}\int_0^{+\infty} N(\Omega)\exp[-j\omega\beta_2(\Omega - \Omega_0)]d\Omega \quad (2)$$

where $N(\Omega)$ is the optical power spectral density (PSD) of the filtered broadband optical source, β_2 is the group velocity dispersion (GVD) of DCF and $\Delta\tau$ is the time delay between the two branches of the MZI. From Eq. (1), the MPF's bandpass center can be expressed by

$$f_c = \Delta\tau/(2\pi\beta_2). \quad (3)$$

As will be shown below, when the loop is connected at the "C" in Fig. 1 (i.e., the close loop), the MPF selects the oscillating frequency of f_c determined by Eq. (3), which can be easily tuned by changing of $\Delta\tau$ or the total dispersion β_2.

Considering a rectangular profile of the optical filter, $N(\Omega)$ can be written by

$$N(\Omega) = \begin{cases} \frac{P_0}{\delta_{3dB}}, & |\Omega - \Omega_0| < \frac{\delta_{3dB}}{2} \\ 0, & |\Omega - \Omega_0| > \frac{\delta_{3dB}}{2} \end{cases} \quad (4)$$

where P_0 is the total power of the optical source and $\delta_{3\,dB}$ the 3-dB optical bandwidth of the sliced BOS, respectively. From Eq. (2) we can deduce

$$H_b(\omega) = \frac{P_0}{2\pi}\frac{\sin(\omega\beta_2\delta_{3dB}/2)}{\omega\beta_2\delta_{3dB}/2}. \quad (5)$$

Fig. 2(a) represents the numerical simulation of the amplitude response [Eq. (5)] under different BOS profile. It is shown that the rectangular profile can better transmit higher frequencies than the Gaussian and Lorentzian profile for the same optical $\delta_{3\,dB}$. The simulated response at different $\delta_{3\,dB}$ of the rectangular profile is illustrated in Fig. 2(b). It decreases with the increase of the RF frequency
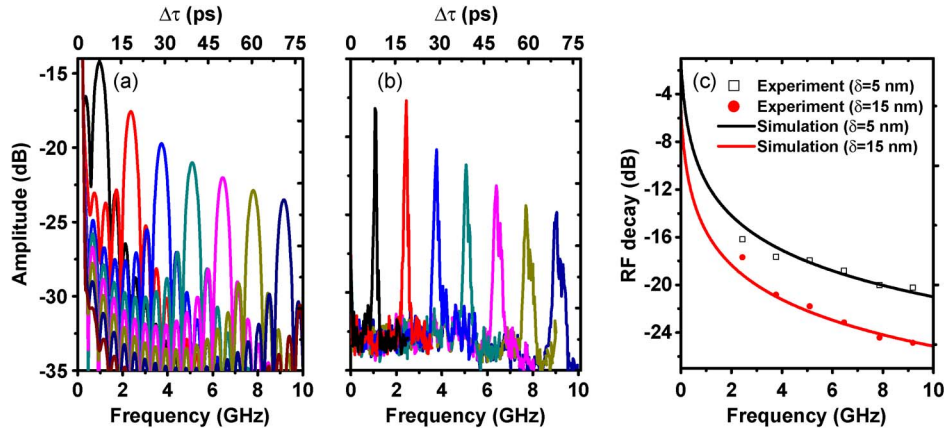
Fig. 3. Simulated (a) and measured (b) MPF frequency response for $\delta_{3\,dB} = 15$ nm rectangular profile. Different colors in (a) or (b) correspond to different frequencies under different delay times $(\triangle\tau)$. (c) The decay effect for $\delta_{3\,dB} = 5$ nm or 15nm.

for a fixed $\delta_{3\,dB}$, and fades when the $\delta_{3\,dB}$ increases from 5 nm to 15 nm at a constant RF frequency of 10 GHz. Fig. 2(c) shows the calculated single-passband RF response under different $\triangle\tau$ in different colors when $\delta_{3\,dB} = 15$ nm, which provides a transmission-null-free property. Besides, there is no broadening of the RF bandwidth due to the rectangular profile of the BOS, which is advantageous for application to higher RF frequency.

However, since the third-order dispersion β_3 of the DCF is non-zero and the width of the sliced BOS is always finite, the MPF suffers more or less the decay effects. Correspondingly, Eq. (1) and Eq. (2) can be rewritten as follows

$$H(\omega) \propto |H_b(\omega)|^2 \propto \frac{2P_0^2}{\delta_{3dB}^2 \omega \beta_3} \tag{6}$$

which demonstrates that more decay occurs for higher frequency and wider $\delta_{3\,dB}$ whatever the filtered BOS is the rectangular profile.

3. Experimental Investigation

The inset of Fig. 1 shows the measured spectrum of the BOS sliced by the optical filter with a rectangular profile. First, the open-loop response of the OEO was detected at the "A" and "B". The optical power fed into the OC1 after amplified is 13 dBm, and the combined power in the OC2 is about 2 dBm due to the optical loss of the VODL and MZM. The dispersive element (DCF) is 8.47-km long and has a total dispersion of $\beta_2 = 1.174 * 10^{-21}$ s^2 and $\beta_3 = 1.293 * 10^{-35}$ s^3. Another EDFA2 laid after the DCF has an optical power of 13 dBm. To avoid the saturation of the 16-GHz PD1 (below 6.5 dBm), an OC3 is used to split 5.4 dBm.

The simulated and measured frequency response as a single MPF for $\delta_{3\,dB} = 15$ nm is compared in Fig. 3(a) and (b), where different colors correspond to different frequencies under different delay times $(\triangle\tau)$. The MPF response was measured by combination of a microwave synthesizer driving the MZM and R&S FSUP signal analyzer serving as an electrical spectrum analyzer (ESA). There are somehow distortions in Fig. 3(b) different from [8] because the scanning step of the microwave synthesizer is about 20 MHz. It is estimated that the insertion loss of the optical link is nearly 16 dB in the low frequency and degrades to 25 dB when the frequency is increased to 10 GHz, which gives a good agreement with the simulation as compared in Fig. 3(c). The coincidence of experiment and simulation of less decay of ~4 dB at less than 10 GHz with narrower band $\delta_{3\,dB}$ of 5 nm is also represented in Fig. 3(c), which verifies that less decay with narrower $\delta_{3\,dB}$ of the theoretical dependence in Eq. (6).
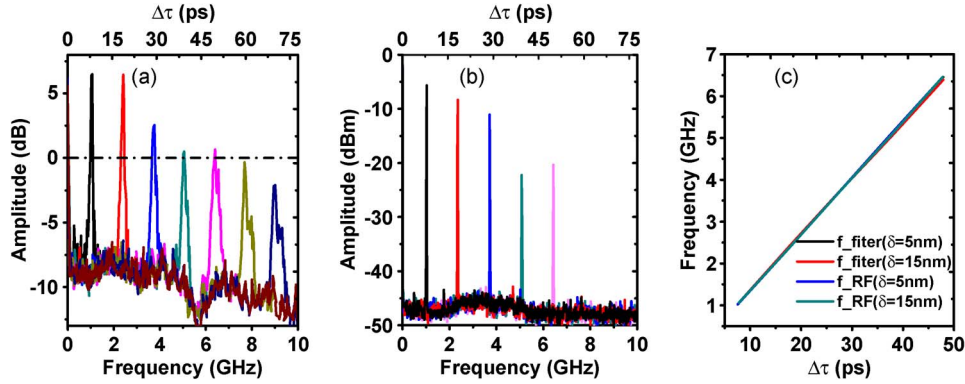
Fig. 4. (a) The filter frequency response after EAP amplified. (b) The generated microwave signals from ~1 GHz to ~6.8 GHz. The resolution bandwidth (RBW) is 300 kHz and $\delta_{3\,dB}$ = 15 nm. Different colors in (a) or (b) correspond to different frequencies under different delay times $(\Delta\tau)$. (c) The tuned filter center frequency (f_filter) and oscillated frequency (f_RF) with the delay of VODL when $\delta_{3\,dB}$ = 5 nm or 15 nm.
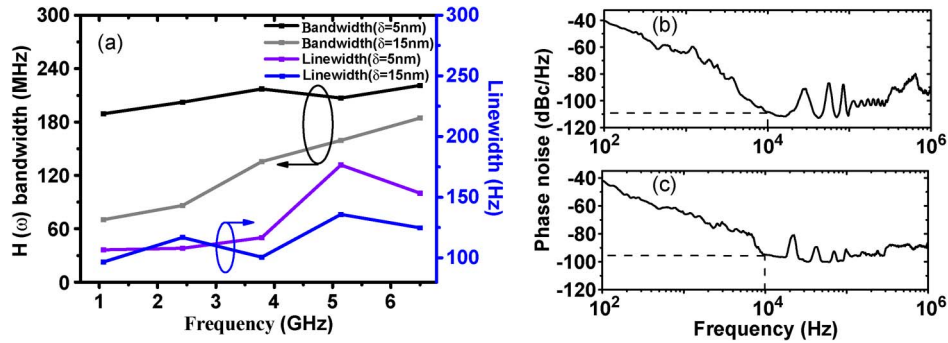

Fig. 5. (a) The linewidth of the generated signal and 3-dB bandwidth of MPF in different $\Delta\tau$ when $\delta_{3\,dB}$ = 5 nm or 15 nm. SSB phase noise spectrum of generated microwave signals at 1.151 GHz (b) and 6.5067 GHz (c), respectively.

Fig. 4(a) shows the frequency response when an electrical amplifier (EAP, gain 22 dB@ DC-10 GHz) is inserted at "C". It can be observed that the link can achieve positive gain when the microwave frequency is less than 7 GHz. Next, we study the close-loop performance of the OEO, i.e., a microwave signal can be generated as long as the oscillation starts. The generated microwave signals from ~1 GHz to ~6.8 GHz with a 1.357-GHz step corresponding to every 10 ps according to Eq. (3) are depicted in Fig. 4(b). It is noted that different colors correspond to different frequencies under different delay times $(\Delta\tau)$. The linear dependence of the tuned filter center as well as the microwave frequency on the corresponding delay $\Delta\tau$ with $\delta_{3\,dB}$ 5 nm and 15 nm is represented in Fig. 4(c), which illustrates that the MPF selects successfully the right mode and the tuned generated microwave is only the function of $\Delta\tau$ (also β_2, but not included in this study). The oscillator can oscillate before 6.8 GHz because the RF insertion loss is higher than 0 dB. It is noted that a maximum frequency of 8.3 GHz can be achieved when the filter $\delta_{3\,dB}$ is tuned to 5 nm due to the less fading [see Fig. 3(c)], which is beyond the first transmission null of 8.235 GHz determined by CSE = $((2k + 1)\pi/\beta_2)^{1/2}$ (k is an integer and $k = 1$ for the first null).

Finally, the linewidth and single-side-band (SSB) phase noise of the oscillating signal are studied. As shown in Fig. 5(a), the linewidth goes broader from ~100 Hz to ~125 Hz with the center frequency (f_c) increasing to ~7 GHz for $\delta_{3\,dB}$ = 15 nm. The broadening effect is more serious for $\delta_{3\,dB}$ = 5 nm. To understand the broadening of linewidth, we measured the 3-dB bandwidth of the single MPF, which is also depicted in Fig. 5(a). It shows that it gets wider with the increasing f_c. This

is because the 3-dB bandwidth increases monotonically with fc due to the effect of the dispersion slope [5]. The bandwidth with $\delta_{3\,dB} = 15$ nm is ~70 MHz at ~1 GHz and it becomes ~230 MHz at ~6.8 GHz, which is similar for the case when the $\delta_{3\,dB}$ is reduced to 5 nm.

The phase noise of the generated signals was also measured by the R&S FSUP signal analyzer. Microwave signals at 1.0612 GHz in Fig. 5(b) and 6.5067 GHz in Fig. 5(c) are for illustration, respectively. The phase noise of the generated microwave signal at an offset frequency of 10 kHz is lower than -110 dBc/Hz at 1.0612 GHz and -95 dBc/Hz at 6.5067 GHz. Several peaks at the resonant frequency of the cavity appear in the offset frequency greater than 20 kHz. The resonant spacing is about 24 kHz, which is identical to the mode spacing of OEO resulted from the non-oscillating side-modes and dedicates the loop is 8.475 km according to $L = c/(n * \Delta f)$ [1], where c is the velocity in the vacuum, n is the effective refractive index of DCF and Δf is the resonant space.

4. Conclusion

A tunable OEO implemented by a CSE-free MPF without using any electronic microwave filters was proposed, and the decay effect of the RF response arising by the interaction between the third-order dispersion and the shaped BOS was deduced. An experiment was demonstrated that the oscillating signal had a tunable range of 6.8 GHz, which is currently limited by the decay effect. A good phase noise performance of nearly -110 dBc/Hz (-95 dBc/Hz) at an offset of 10 kHz for the RF frequency of ~1.06 GHz (~6.5 GHz) was achieved. It is expectable to extend the oscillating frequency of the OEO if an electronic amplifier is replaced by a low noise amplifier with higher gain or using the non-uniformly slicing the BOS [9] or compensating the dispersive slope by cascading opposite-slope elements [15]. It is now under plan to stabilize the OEO by use of Vernier effect [16] since there exists the mode hopping effect due to the mismatching between the single bandpass MPF's bandwidth (hundreds of MHz) and the cavity's mode spacing (tens of kHz).

References

[1] X. S. Yao and L. Maleki, "Optoelectronic microwave oscillator," *J. Opt. Soc. Amer. B, Opt. Phys.*, vol. 13, no. 8, pp. 1725–1735, Aug. 1996.
[2] D. Eliyahu and L. Maleki, "Tunable, ultra-low phase noise YIG based opto-electronic oscillator," in *Proc. IEEE MTT-S Int. Microw. Symp. Dig.*, 2003, pp. 2185–2187.
[3] W. Li and J. Yao, "An optically tunable optoelectronic oscillator," *J. Lightwave Technol.*, vol. 28, no. 18, pp. 2640–2645, Sep. 2010.
[4] D. Strekalov, D. Aveline, N. Yu, R. Thompson, A. B. Matsko, and L. Maleki, "Stabilizing an optoelectronic microwave oscillator with photonic filters," *J. Lightwave Technol.*, vol. 21, no. 12, pp. 3052–3061, Dec. 2003.
[5] J. Mora, B. Ortega, A. Díez, J. L. Cruz, M. V. Andrés, J. Capmany, and D. Pastor, "Photonic microwave tunable single-bandpass filter based on a Mach–Zehnder interferometer," *J. Lightwave Technol.*, vol. 24, no. 7, pp. 2500–2509, Jul. 2006.
[6] T. X. Huang, X. Yi, and R. A. Minasian, "Single passband microwave photonic filter using continuous-time impulse response," *Opt. Exp.*, vol. 19, no. 7, pp. 6231–6242, Mar. 2011.
[7] W. Li, M. Li, and J. Yao, "A narrow-passband and frequency-tunable microwave photonic filter based on phase-modulation to intensity-modulation conversion using a phase-shifted fiber Bragg grating," *IEEE Trans. Microw. Theory Tech.*, vol. 60, no. 5, pp. 1287–1296, May 2012.
[8] X. Xue, X. Zheng, H. Zhang, and B. Zhou, "Widely tunable single-bandpass microwave photonic filter employing a non-sliced broadband optical source," *Opt. Exp.*, vol. 19, no. 19, pp. 18 423–18 429, Sep. 2011.
[9] X. Yi and R. Minasian, "Dispersion induced RF distortion of spectrum-sliced microwave-photonic filters," *IEEE Trans. Microw. Theory Tech.*, vol. 54, no. 2, pp. 880–886, Feb. 2006.
[10] S. Pan and J. Yao, "Wideband and frequency-tunable microwave generation using an optoelectronic oscillator incorporating a Fabry–Perot laser diode with external optical injection," *Opt. Lett.*, vol. 35, no. 11, pp. 1911–1913, May 2010.
[11] B. Yang, X. Jin, X. Zhang, S. Zheng, H. Chi, and Y. Wang, "A wideband frequency-tunable optoelectronic oscillator based on a narrowband phase-shifted FBG and wavelength tuning of laser," *IEEE Photon. Technol. Lett.*, vol. 24, no. 1, pp. 73–75, Jan. 2012.
[12] M. Li, W. Li, and J. Yao, "Tunable optoelectronic oscillator incorporating a high-Q spectrum-sliced photonic microwave transversal filter," *IEEE Photon. Technol. Lett.*, vol. 24, no. 14, pp. 1251–1253, Jul. 2012.
[13] X. Liu, W. Pan, X. Zou, B. Luo, L. Yan, and B. Lu, "A reconfigurable optoelectronic oscillator based on cascaded coherence-controllable recirculating delay lines," *Opt. Exp.*, vol. 20, no. 12, pp. 13 296–13 301, Apr. 2012.

[14] V. J. Urick, M. E. Godinez, P. S. Devgan, J. D. McKinney, and F. Bucholtz, "Analysis of an analog fiber-optic link employing a low-biased Mach–Zehnder modulator followed by an erbium-doped fiber amplifier," *J. Lightwave Technol.*, vol. 27, no. 12, pp. 2013–2019, Jun. 2009.

[15] J. H. Lee, Y. M. Chang, and S. B. Lee, "Spectrum slicing-based, high-Q, photonic microwave filter using the combination of incoherent continuous-wave supercontinuum and dispersion-profiled fiber," presented at the OFC/NFOEC, San Diego, CA, USA, 2008, Paper OThH4.

[16] Z. Tang, S. Pan, D. Zhu, R. Guo, Y. Zhao, M. Pan, D. Ben, and J. Yao, "Tunable optoelectronic oscillator based on a polarization modulator and a chirped FBG," *IEEE Photon. Technol. Lett.*, vol. 24, no. 17, pp. 1487–1489, Sep. 2012.